9-18-1995

Magnetic-Field-Induced Griffiths Phase versus Random-Field Criticality and Domain Wall Susceptibility of Fe0.47Zn0.53F2

Christian Binek
University of Nebraska-Lincoln, cbinek@unl.edu

S. Kuttler
Angewandte Physik, Gerhard-Mercator-Universitat, Duisburg, Germany

Wolfgang Kleemann
Angewandte Physik, Gerhard-Mercator-Universitat, Duisburg, Germany, wolfgang.kleemann@uni-due.de

Magnetic-Field-Induced Griffiths Phase versus Random-Field Criticality and Domain Wall Susceptibility of $Fe_{0.47}Zn_{0.53}F_2$

Ch. Binek, S. Kuttler, and W. Kleemann
Angewandte Physik, Gerhard-Mercator-Universität Duisburg, D-47048 Duisburg, Germany
(Received 10 May 1995)

The well-known peak of the parallel ac susceptibility arising below T_N in $Fe_{0.47}Zn_{0.53}F_2$ splits into a narrow critical peak at $T_c(H)$ and a broad field-induced Griffiths phase shoulder peaking at $T_p > T_c(H)$ in magnetic fields $H \gtrsim 1.6$ MA/m. Random-field (RF) criticality with $\tilde{\alpha} \approx 0$ and subsequent rounding due to RF trapping of thermal fluctuations are observed upon zero-field cooling as $T \to T_c^-(H)$. The frozen domain state obtained after rapid field cooling reveals excess susceptibility $\Delta\chi_w' \propto H^{2.6}$, owing to rough walls with thermally activated stiffness.

PACS numbers: 75.40.Cx, 75.40.Gb, 75.50.Lk, 75.60.Ch

In the recent years uniaxial antiferromagnets (AF's) in an external axial magnetic field $H = H_0$ have often been used as model systems for two very different critical point scenarios. On one hand, a three-dimensional diluted AF in a field (DAFF) is expected [1] to reveal the critical behavior of the random-field Ising model (RFIM) [2]. In fact, the static critical exponents obtained on DAFF systems like $Fe_{1-x}Zn_xF_2$, $x > 0$ [3] come close to those obtained, e.g., on the structural RFIM system $DyAs_{1-x}V_xO_4$, $x > 0$ [4]. On the other hand, H_0 induces a Griffiths-like phase in Ising-type antiferromagnets like $FeCl_2$ [5] and $FeBr_2$ [6] within the temperature range $T_c(H_0) \equiv T_c \leq T \leq T_c(H = 0) \equiv T_N$. Fluctuations of the field-induced magnetization give rise to local changes of the magnetic field $0 \leq H \leq H_0$ and hence to "local" phase transitions (PT's), distributed smoothly throughout the above temperature range. An infinite series of weak singularities arises by analogy with the original Griffiths phase [7] in a diluted ferromagnet at $H_0 = 0$ within $T_c(x) \leq T \leq T_c(x = 0)$ as evidenced by susceptibility measurements on $K_2Cu_{0.8}Zn_{0.2}F_4$ and $F_{0.47}Zn_{0.53}F_2$ only recently [8].

In this Letter we consider for the first time the simultaneous appearance of both RFIM criticality and Griffiths-type pseudocriticality in a DAFF system, $Fe_{0.47}Zn_{0.53}F_2$, based on ac susceptibility data, χ' vs T, in dependence on H_0 and frequency f, respectively. First of all, we show that the field-induced peak of χ' vs T, which was previously [9] attributed to RFIM criticality, primarily reflects the pseudocritical response of the field-induced Griffiths phase (henceforth denoted as the Griffiths peak). In large enough fields, $H_0 \gtrsim 1.6$ MA/m, a narrow peak splits off just below the Griffiths peak temperature $T_p(H_0) \equiv T_p$. Its low-T slope reflects RFIM critical behavior with a specific heat exponent $\tilde{\alpha} \approx 0$, in accordance with most experiments [3]. Rounding of this peak at $|t| < 10^{-2}$, where $t = (T - T_c)/T_N$, corroborates the suspected [10] destruction of the PT, owing to irreversible trapping of the AF order parameter at spatial RF fluctuations in agreement with computer simulations [11] and recent experiments [12,13]. Finally, in the static domain state [14] obtained well below T_c after rapid field cooling (FC), we observe for the first time the excess susceptibility of domain walls $\Delta\chi_w$, which scales with H_0 as the excess wall magnetization ΔM [14,15].

Susceptibility χ' vs T, was measured with a superconducting quantum interference device (SQUID) susceptometer (Quantum Design MPMS-5S) at temperatures $10 \leq T \leq 50$ K, fields $H_0 \leq 4$ MA/m, ac field amplitudes $\Delta H = 320$ A/m, and frequencies $0.05 \leq f \leq 500$ Hz. Temperatures were stabilized to within $\Delta T = \pm 0.01$ K. The very small concentration gradient of the sample [16] causes minimal spread of local critical temperatures, $|\Delta T_c| < 0.03$ K, over its total volume of $\approx 2 \times 2 \times 3\ \mathrm{mm}^3$. This is confirmed by comparing SQUID and locally resolved Faraday rotation measurements [9] of χ' vs T on comparable samples at $H_0 = 0.08$ MA/m and $f = 0.02$ Hz.

Figure 1 shows χ' vs T, as obtained with $f = 1$ Hz and $H_0 = 0.8$, 1.6, 2.4, 3.2, and 4 MA/m, upon FC

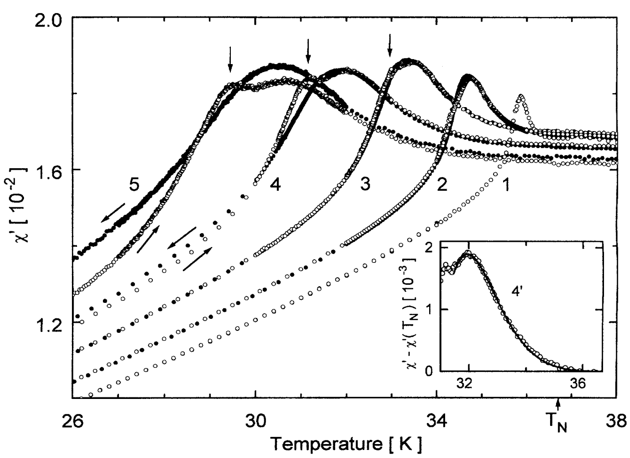

FIG. 1. χ' vs T measured at $f = 1$ Hz and (1) $H_0 = 0.8$, (2) 1.6, (3) 2.4, (4) 3.2, and (5) 4 MA/m upon ZFC-FH (open circles, arrow) and FC (solid circles, arrow), respectively. T_N and various $T_c(H_0)$ are indicated by vertical arrows. The solid line fitted to the partially shown ZFC-FH data of $\chi' - \chi'(T_N)$ for $H_0 = 3.2$ MA/m (inset, curve 4′) refers to Eq. (4).

and field heating (FH) after zero-field cooling (ZFC), respectively. The field-induced peak [9] appearing below $T_N = 36.70$ K broadens considerably when increasing H_0. Only upon ZFC-FH and at $H_0 \geq 2.4$ MA/m does it split into a broad main and a narrow low-T peak at T_c, a novel feature which becomes most pronounced at high fields. On the other hand, the ZFC-FH curves fall below the FC ones to both sides of the novel extra peak, as seen most drastically for $H_0 = 4$ MA/m.

The broad main peak is supposed to reflect the field-induced weak Griffiths-type singularities expected between T_N and T_c. We introduce a phenomenological Lorentzian distribution of local critical temperatures T_c' [17],

$$P(T_c' T) = \varepsilon / \{[\varepsilon^2 + (T_c - T_c')^2] \arctan[(T_N - T_c)/\varepsilon]\}, \quad (1)$$

with $T_c \leq T_c' \leq T_N$ and $\varepsilon > 0$. We use the scaling behavior of the real part of the susceptibility [18],

$$\chi_c' = A^{\pm} H^y - |T - T_c'|^{-\tilde{\alpha}} \quad (A^+, A^- = \text{const}), \quad (2)$$

where $y = (2/\phi)(2 + \tilde{\alpha} - \alpha - \phi)$; $\tilde{\alpha}$, α, and ϕ are the amplitude, RFIM, random exchange Ising model (REIM), and crossover exponents, respectively [18]. $H(T_c')$ is obtained from [3]

$$T_c'(H) = T_N - BH^2 - AH^{2/\phi} \; (A, B = \text{const}). \quad (3)$$

The weighted susceptibility is then

$$\chi'(T) \propto \int_{T_c}^{T_N} dT_c' P(T_c', T) \chi'(T_c', T)$$
$$\approx \chi'(T_N) + \varepsilon (T_N - T)^{y\phi/2} (A^+ |T - T_c|^{1-\tilde{\alpha}} + A^- |T_N - T|^{1-\tilde{\alpha}}) / \{(1 - \tilde{\alpha})[\varepsilon^2 + (T_c - T)^2] \arctan[(T_N - T_c)/\varepsilon]\}. \quad (4)$$

$\chi'(T_N)$ is the constant regular background. As expected, in this zeroth-order approximation, the singularities [Eq. (2)] are averaged out. We note that Eq. (4) requires $\tilde{\alpha} \geq 0$, unless a cusp height is introduced as an additional constant in Eq. (2).

Anticipating $\tilde{\alpha} = 0$ (see below) and employing $\chi'(T_N)$, $b = \varepsilon T$, A^+, A^-, T_c, and $y\phi/2$ as fitting parameters, we obtain nearly perfect fits to Eq. (4) of the experimental ZFC-FH data as shown for $H_0 = 3.2$ MA/m within $31.34 \leq T \leq T_N$ (solid line in Fig. 1, inset). In particular, the broad peak at $T_p = 32.0$ K is perfectly modeled. $T_c = 31.47$ K lies close to the experimental value 31.13 K (see Fig. 3). Best fits to nine χ' vs T curves for $1.6 \leq H_0 \leq 4$ MA/m reveal a power law $b = b_0 H_0^{\delta}$, with $b_0 = 11.0$ K^2 and $\delta = 1.38 \pm 0.24 \approx 2/\phi$, where $\phi = 1.42$ [3]. Comparison with Eq. (3), neglecting the small [3] mean-field correction BH^2, reveals a remarkable proportionality $b \propto T_N - T_c$. It indicates small, but finite b values in the low-H_0 regime, where both Griffiths-type precursors and the critical singularity superimpose in unresolved peaks. This raises doubts about critical point analysis in this region [9], which should be carefully reconsidered. Below, it will be shown how to extract in a more reliable manner critical exponents at larger fields $H_0 \geq 2.8$ MA/m.

It should be noted that the distribution function [Eq. (1)] does not account for the appearance of criticality at $T_c' = T_c$, which refers to an infinite static cluster and $H = H_0$. More complete analysis would require an additional deltalike probability ($b \rightarrow 0$) in Eq. (1), the weight of which is complementary to that of the dynamic clusters in the Griffiths precursor region. Traces of the novel critical peak splitting off at T_c from the low-T shoulder of χ' vs T were already visible in previous work at $H_0 = 0.8 - 1.6$ MA/m, but remained unnoticed [9]. It was remarked, however, that the imaginary part, χ'' vs T, is much narrower than the total χ' anomaly [9]. Our data (not shown) reveal a sharp peak of χ'' at T_c, which coincides with the critical χ' analog. It extends an asymmetric flat tail throughout the Griffiths phase region similar to previous observations [5,6].

Figure 2 shows χ' vs T data obtained with $H_0 = 3.4$ MA/m after ZFC-FH (curve 1) and after FC (curve 2), respectively. Obviously, the critical singularity $\Delta\chi_c'$ is only present in curve 1 owing to the AF long-range order (LRO) prepared at $T < T_c$. The absence of $\Delta\chi_c'$ in curve 2 is due to the well-known [3,14] dynamic freezing of the DAFF system into an AF domain state. We interpret

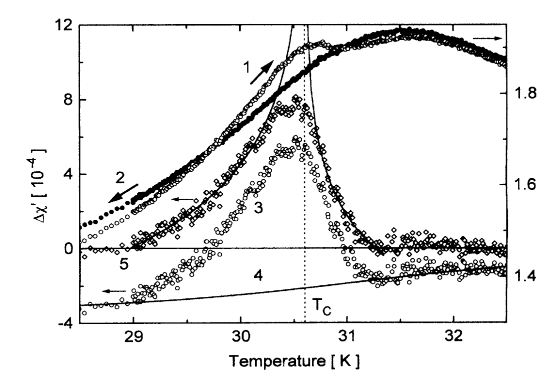

FIG. 2. χ' vs T (right-hand scale) measured at $f = 1$ Hz and $H_0 = 3.4$ MA/m upon (1) ZFC-FH and (2) FC, their difference (3) $\Delta\chi'$ vs T (left-hand scale) decomposed into (curve 4) $\Delta\chi_w'(T)$ and (curve 5) $\Delta\chi_c'(T)$, with logarithmic singularity (solid lines) best-fitted within $29.0 < T < 30.2$ K and $30.7 < T < 31.4$ K, where $T_c = 30.60$ K (dashed line).

the difference curve 3, $\Delta\chi' = \chi'$(ZFC-FH) $-\chi'$(FC), as a critical peak with half-width $\Delta T_{12} < 1$ K, however, still showing negative tails outside the peak region. These are due to extra contributions to χ'(FC) of domain walls $\Delta\chi'_w$. Similarly, as in the related ΔM effect [14], they establish upon FC at $T \le T_{eq} \approx 32$ K, where $\Delta\chi'$ starts to decrease. Only within the temperature range $29.7 \le T \le 31.0$ K are the wall contributions outweighed by the critical ones. By fitting the wings of curve 3 to an empirical function, $\Delta\chi'_w = c_1 \arctan[c_2(T - c_3)] + c_4T + c_5$ with appropriate parameters $c_1, \ldots, c_5$, we are able to model the wall susceptibility (curve 4). The arctan function accounts for the smooth step rising between T_c and T_{eq} [14]. The critical anomaly, $\Delta\chi'_c = \Delta\chi' - \Delta\chi'_w$, thus obtained (curve 5) asymptotically vanishes far from the critical region. Essentially, the same result emerges when replacing our extensive stepwise data manipulation by immediate subtraction of an empirical noncritical background [9] from curve 1. Albeit being ill-defined, such a procedure might serve for cross-checking purposes.

Scaling considerations [9,18] predict $\Delta\chi'_c = B^{\pm}|t|^{-\tilde{\alpha}}$ with amplitudes $B^{\pm}$. Separate fitting procedures, inserting $\tilde{\alpha} > 0$ and $\tilde{\alpha} < 0$ (requiring an additional constant for the cusp height), indicate convergence to $\tilde{\alpha} \approx 0$, i.e., to logarithmic singularities as obtained from other experiments on DAFF systems [3]. This is shown by the solid lines in Fig. 2 for the data at $H_0 = 3.4$ MA/m, best-fitted within $-0.05 \le t \le -0.01$ and $0.003 \le t \le 0.02$, where $T_c = 30.60$ K. $T_c(H_0)$, thus obtained at $H_0 = (2.8 + n \cdot 0.2)$ MA/m, $0 \le n \le 6$, varies according to Eq. (3) with a reasonable [3] best-fit exponent $\phi = 1.40 \pm 0.03$. A full account of the static critical behavior will be given elsewhere. In particular, the unusually [3] small amplitude ratio $B^+/B^- = 0.74 \pm 0.05$ has to be discussed in more detail. It seems to hint at a remaining interference of $\Delta\chi'_c$ with Griffiths-type noncritical contributions at $t > 0$.

Above $t \approx -0.01$, i.e., outside the concentration-induced spread of $|\Delta T_c|T_N \approx 10^{-3}$, the critical peak breaks off into a flat plateau. According to early computer simulations [11], considerations of the tremendous critical slowing down of the RFIM [19], and recent scaling theory [10], both RFIM and DAFF systems are supposed to fall out of equilibrium on approaching T_c. Increasingly larger thermal fluctuations of the AF order parameter become trapped at spatial fluctuations of the RF's. A domain state is expected to occur even in a ZFC-FH process [10]. It might also explain the anomalous drop of the x-ray scattering intensity observed on $Mn_{0.75}Zn_{0.25}F_2$ [12] and $Fe_{0.5}Zn_{0.5}F_2$ [13] as $T \to T_c^-$. The situation is, however, far from being fully understood. For example, criticality is not excluded in the infinite waiting time limit of the domain state merely represents local minima of the free energy. Alternatively, a first-order PT [20] or a spin-glass phase [21] might be involved.

$\Delta\chi'_c$ vs T, measured upon ZFC-FH at $H_0 = 3.2$ MA/m and various frequencies $0.05 \le f \le 500$ Hz, clearly reveals dynamic broadening [Fig. 3(a)]. The amplitudes of the best-fitted logarithmic singularities decrease with increasing f, as expected from dynamic scaling (see below). This has to be distinguished from the (party asymmetric) plateaus occurring in all curves at $t \approx -0.01$, where $T_c = (31.13 \pm 0.01)$ K. They are due to irreversibility on a time scale beyond our largest reciprocal frequency $1/f \le 20$ s, as argued above.

Conventional dynamic scaling theory predicts [9] data collapsing of $\Delta\chi'_c$ vs T in a plot of $\Delta\chi'_c/\log_{10}(f/f_0)$ vs $|t| \cdot (f/f_0)^{-1/z\nu}$, if $\tilde{\alpha} = 0$, where z and ν are the dynamic and the correlation-length critical exponents of the RFIM. This is quite reasonably demonstrated in Fig. 3(b) by best-fitting the data of Fig. 3(a) for $T < T_c$, with $f_0 = 10^9$ Hz and $z\nu = 14$. The value of f_0 is consistent with the slow dynamics of the REIM [3]. The unusually large value of $z\nu$ might hint at activated critical dynamics proposed of both DAFF [9] and RFIM [19], and will be discussed in greater detail elsewhere.

The predicted [22] excess wall susceptibility, $\Delta\chi'_w$, observed after FC was hitherto denied occurrence in DAFF systems [9]. In fact, as shown in Fig. 4, $\Delta\chi'_w$ virtually vanishes at $H_0 < 1.6$ MA/m after slow FC to low temperatures $10 \le T \le 25$ K (solid circles). Formally obeying a power law, $\Delta\chi'_w \propto H^{6.5}$, it rises steeply only at $H_0 > 2.4$ MA/m. Rapid quenching however, from $T = 2T_c$ to $T_c - 10$ K increases $\Delta\chi'_w$ considerably (open circles), since domain wall relaxation toward LRO taking place just below T_c [14] is largely suppressed. $\Delta\chi'_w \propto 1/R(H_0)$ [22] is related to the radius of the smallest RF-induced domains $R(H_0) \propto H_0^{-\mu}$, where $\mu = 2$ for compact domains [19]. Our data are best-fitted by a power law $\Delta\chi'_w \propto H^{\mu}$, the exponent of which, $\mu = 2.6 \pm 0.3$

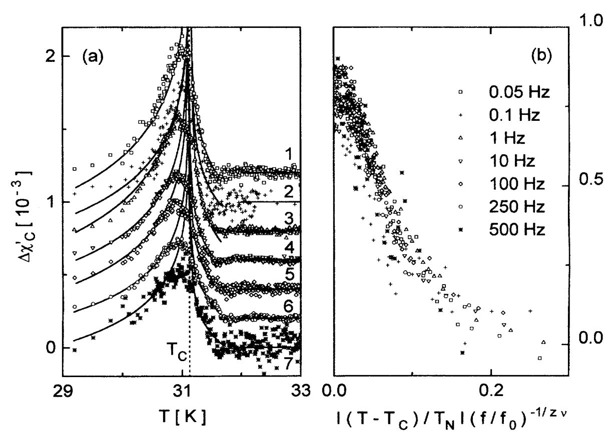

FIG. 3. (a) $\Delta\chi'_c$ vs T obtained as in Fig. 2 at $H_0 = 3.2$ MA/m and (1) $f = 0.05$, (2) 0.1, (3) 1, (4) 10, (5) 100, (6) 250, and (7) 500 Hz, shifted successively by amounts of 2×10^{-4} (horizontal lines), and best-fitted within $29.2 < T < 30.7$ K and $31.2 < T < 31.6$ K by logarithmic singularities (solid curves). $T_c = 31.13$ K is indicated by a vertical dashed line. (b) Dynamic scaling plot of the data of (a) shown with identical symbols (see text).

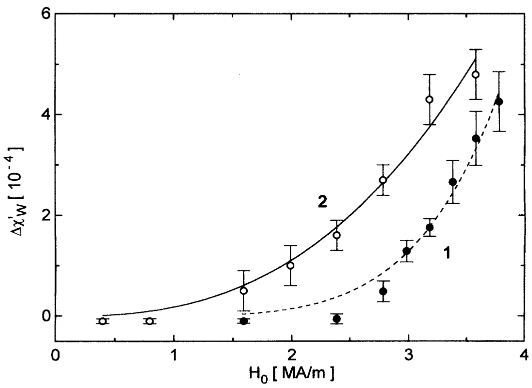

FIG. 4. $\Delta\chi'_w$ vs H_0 obtained after slow (solid circles, $-dT/dt \approx 2 \times 10^{-5}$ K/s, averaged within $10 \leq T \leq 25$ K) and after rapid FC to $T_c - 10$ K (open circles, $-dT/dt \approx 0.5$ K/s, averaged over five measurements) and best-fitted to power laws, $\Delta\chi'_w \propto H_0^\mu$ [**1**, $\mu = 6.5$ (dashed line); **2**, $\mu = 2.6$ (solid line)], respectively.

(solid line), signifies fractality of the domain walls [23] in accordance with magnetization data of $Fe_{0.5}Zn_{0.5}F_2$ [15]. It is interesting to note that $\Delta\chi'_w$ decreases linearly with T when cooling the sample to below the quenching temperature (not shown). This is probably due to a thermally activated decrease of the wall stiffness Γ, owing to weakening of the pinning forces with increasing T, since $\Delta\chi'_w \propto 1/\Gamma$ [22].

In conclusion, we have shown that the dynamically rounded peak of $\chi'(T)$ at $T_p < T_N$ in the DAFF system $Fe_{0.47}Zn_{0.53}F_2$ originates primarily from the field-induced Griffiths phase. AT $H \gtrsim 1.6$ MA/m, a weak singularity splits off at $T_c < T_p$. In the sense of a sum rule, it involves only a small portion of the spin system. A similar explanation might apply to the anomalously small singularity of the specific heat [3,13]. The critical exponent $\tilde{\alpha} \approx 0$ corroborates other experiments. It remains to be explored, why, e.g., the symmetric logarithmic divergence of $(\partial M/\partial T)_H$ vs T [3,13] seems to be much less influenced by the Griffiths phase than our highly asymmetric $\chi'(T)$ curve.

Extremely slow critical dynamics is reflected by the frequency dependence of χ', and, in addition, by the breaking away of the critical peak very near to T_c. The question is still open; if this implies near-tricriticality [20], an intermediate domain state [10], or a new phase with spin-glass LRO [21]. Fractal domain wall susceptibility, $\Delta\chi'_w \propto H^{2.6}$, is observed after rapid FC to low temperatures. Logarithmic frequency dispersion [22] and independence of T in the quantum tunneling regime ($T \rightarrow 0$) are expected, and presently under investigation.

Fruitful discussions with D. P. Belanger are gratefully acknowledged. This was supported by the Deutsche Forschungsgemeinschaft through Sonderforschungsbereich 166.

[1] S. Fishman and A. Aharony, J. Phys. C **12**, L729 (1979); J. L. Cardy, Phys. Rev. B **29**, 505 (1984).
[2] Y. Imry and S. K. Ma, Phys. Rev. Lett. **35**, 1399 (1975).
[3] D. P. Belanger and A. P. Young, J. Magn. Magn. Mater. **100**, 272 (1991), and references therein.
[4] J. T. Graham, J. H. Page, and D. R. Taylor, Phys. Rev. B **44**, 4127 (1991).
[5] Ch. Binek and W. Kleemann, Phys. Rev. Lett. **72**, 1287 (1994).
[6] Ch. Binek, M. M. P. de Azevedo, D. Bertrand, and W. Kleemann, J. Magn. Magn. Mater. **140-144**, 1555 (1995).
[7] R. B. Griffiths, Phys. Rev. Lett. **23**, 17 (1969).
[8] Ch. Binek and W. Kleemann, Phys. Rev. B **51**, 12 888 (1995).
[9] A. R. King, J. Mydosh, and V. Jaccarino, Phys. Rev. Lett. **56**, 2525 (1986); A. E. Nash, A. R. King, and V. Jaccarino, Phys. Rev. B **43**, 1272 (1991).
[10] Y. Shapir, in *Recent Progress in Disordered Magnetism,* edited by D. H. Ryan (World Scientific, Singapore, 1992), p. 309.
[11] H. Yoshizawa and D. P. Belanger, Phys. Rev. B **30**, 5220 (1984).
[12] J. P. Hill, Q. Feng, R. J. Birgeneau, and T. R. Thurston, Z. Phys. B **92**, 285 (1993).
[13] R. J. Birgeneau, Q. Feng, Q. J. Harris, J. P. Hill, A. P. Ramirez, and T. R. Thurston, Phys. Rev. Lett. **75**, 1198 (1995).
[14] W. Kleemann, Int. J. Mod. Phys. B **7**, 2469 (1993), and references therein.
[15] Q. Feng, R. J. Birgeneau, and J. P. Hill, Phys. Rev. B **51**, 15 188 (1995).
[16] The sample was grown by N. Nighman, University of California, Santa Barbara, and kindly provided by V. Jaccarino.
[17] Ch. Binek and W. Kleemann, Acta Phys. Pol. B **44**, 435 (1994).
[18] W. Kleemann, A. R. King, and V. Jaccarino, Phys. Rev. B **34**, 479 (1986).
[19] J. Villain, J. Phys. (Paris) **46**, 1843 (1985); D. S. Fisher, Phys. Rev. Lett. **56**, 416 (1986).
[20] A. Aharony, Phys. Rev. B **18**, 3316, 3328 (1978); H. Rieger and A. P. Young, (to be published).
[21] M. Mezard and R. Monasson, Phys. Rev. B **50**, 7199 (1994).
[22] T. Nattermann, Y. Shapir, and I. Vilfan, Phys. Rev. B **42**, 8577 (1990).
[23] U. Nowak and K. D. Usadel, Phys. Rev. B **44**, 7426 (1991).